Accelerated hepatocellular carcinoma development in mice expressing the Pim-3 transgene selectively in the liver

Accelerated hepatocellular carcinoma development in mice expressing the Pim-3 transgene selectively in liver

Yu Wu,[1, 2] Ying Ying Wang,[2] Yasunari Nakamoto,[3] Ying-Yi Li,[2, 4] Tomohisa Baba,[2] Shuichi Kaneko,[3] Chifumi Fujii,[2, 6] and Naofumi Mukaida[2, 5]

[1] Department of Hematology and Hematology research Laboratory, State Key Laboratory of Biotherapy and Cancer Center, West China Hospital, Sichuan University, Chengdu, Sichuan Province 610041, China, [2] Division of Molecular Bioregulation, Cancer Research Institute, Kanazawa University, 13-1 Takara-machi, Kanazawa 920-0934, Japan, [3]Department of Disease Control and Homeostasis, Graduate School of Medical Sciences, Kanazawa University, 13-1 Takara-machi, Kanazawa 920-8640, Japan, [4]Researcher Center, Fudan University Cancer Hospital, Shanghai, 200032, China.

[5]All correspondence should be addressed to Naofumi Mukaida, MD, PhD, Division of Molecular Bioregulation, Cancer Research Institute, Kanazawa University, 13-1 Takara-machi, Kanazawa 920-0934, Japan.
Tel: 81-76-265-2767 Fax: 81-76-234-4520
E-mail: naofumim@kenroku.kanazawa-u.ac.jp

[6]Present address, Department of Integrative Physiology, School of Medicine, Shinshu University, 3-1-1 Asahi, Matsumoto 390-8621, Japan

Running title: Hepatocellular carcinoma in Pim-3 transgenic mice

Keywords: serine/threonine kinase, apoptosis, cell cycle, Bad

Abstract

Pim-3, a proto-oncogene with serine/threonine kinase activity, was enhanced in hepatocellular carcinoma (HCC) tissues. In order to address the roles of Pim-3 in HCC development, we prepared transgenic mice, which express human Pim-3 selectively in liver. The mice were born at a Mendelian ratio, were fertile and did not exhibit any apparent pathological changes in the liver until one year after birth. Pim-3-transgenic mouse-derived hepatocytes exhibited accelerated cell cycle progression. The administration of a potent hepatocarcinogen, diethylnitrosamine (DEN), induced accelerated proliferation of liver cells in Pim-3 transgenic mice in the early phase, compared to that observed for wild-type mice. DEN treatment induced lipid droplet accumulation with increased proliferating cell numbers 6 months after the treatment. Eventually, wild-type mice developed HCC with a frequency of 40 % until 10 month after the treatment. Lipid accumulation was accelerated in Pim-3 transgenic mice with higher proliferating cell numbers, compared to that observed for wild-type mice. Pim-3 transgenic mice developed HCC with a higher incidence (80 %) and a heavier burden, together with enhanced intratumoral CD31-positive vascular areas, compared to that observed for wild-type mice. These observations indicate that Pim-3 alone cannot cause, but can accelerate HCC development when induced by a hepatocarcinogen like DEN.

Introduction

There were over 667,000 new cases of hepatocellular carcinoma (HCC) worldwide in 2005. The 5-year survival rate of individuals with hepatic malignancy is only 8.9 % despite aggressive conventional therapy, making hepatic malignancy the second most lethal cancer among human malignancies (Farazi and DePinho, 2006; Umemura *et al.*, 2009). HCC usually arises in conditions, that can cause liver cirrhosis, such as chronic hepatitis B and C viral infection, chronic alcohol consumption, and intake of food contaminated with aflatoxin-B_1 (Zheng *et al.*, 2007). These conditions generally provoke continuous rounds of hepatocyte damage in the setting of chronic hepatitis or liver cirrhosis, and eventually activate resident or inflammatory non-parenchymal cells to produce growth factors and cytokines (Otani *et al.*, 2005). The produced factors can drive compensatory and aberrant proliferation of surviving hepatocytes and development of pre-malignant dysplastic nodules, which form the nucleus of neoplastic lesions. Only recently has the molecular analysis of human HCC unraveled many genetic and epigenetic alterations that result in the deregulation of key proto-oncogenes and tumor-suppressor genes including TP53, β-catenin, ErbB receptors family members, *met* and its ligand, hepatocyte growth factor (HGF), p16, E-cadherin and cyclooxygenase 2 (COX2) (Hosono *et al.*, 1993). However, the roles of other proto-oncogenes and tumor suppressor genes in HCC development still remain elusive (Thorgeirsson and Grisham, 2002).

We previously identified Pim-3, a proto-oncogene with serine/threonine kinase activity, as the gene selectively expressed in pre-malignant and malignant lesions of the mouse HCC model in HBV surface antigen transgenic mice (Fujii *et al.*, 2005). Pim-3 was originally identified as a depolarization-induced gene, KID-1 in PC12 cells, a rat pheochromocytoma cell line (Feldman *et al.*, 1998). Subsequently, Deneen and colleagues demonstrated that Pim-3 gene transcription was enhanced in the EWS/ETS-induced malignant transformation of NIH 3T3 cells (Deneen *et al.*, 2003), suggesting the involvement of Pim-3 in tumorigenesis. Consistently, we observed that Pim-3 expression was enhanced in carcinomas but not in normal tissues of human endoderm-derived organs including liver (Fujii *et al.*, 2005), pancreas (Li *et al.*, 2006), colon (Popivanova *et al.*, 2007), and stomach

(Zheng *et al.*, 2008). Moreover, Pim-3 can inactivate a pro-apoptotic molecule, Bad, and maintain the expression of an anti-apoptotic molecule, Bcl-X_L, and prevent apoptosis of human pancreatic cancer and colon cancer cells (Li *et al.*, 2006). Likewise, the ablation of endogenous Pim-3 by short interfering RNA reduced the cell growth of human HCC cell lines by inducing their apoptosis (Fujii *et al.*, 2005).

These observations prompted us to investigate the effects of liver-specific Pim-3 overexpression on HCC development. Although we could not observe spontaneous HCC development in liver-specific Pim-3 transgenic mice, these mice developed HCC with a higher incidence and a heavier hepatocarcinoma burden, when a potent hepatocarcinogen, diethylnitrosamine (DEN) was administered during the suckling period. These results suggest that Pim-3 can accelerate but is not likely the primary inducer of HCC development.

Materials and Methods

Preparation of Pim-3 transgenic mice

The mouse albumin enhancer/promoter region (Fig. 1A) was a kind gift of Dr. Palmiter (University of Washington, Seattle, WA, USA) (Pinkert *et al.*, 1987). Full-length human *Pim-3* cDNA was subcloned 3' to this albumin enhancer/promoter gene. After being linearized by digestion with Not I, the gene was introduced into fertilized oocytes of C57BL/6 using a standard transgenic technique. Genomic DNA was isolated from the tail of the founder and offspring using Nucleospin tissue kit (Macherey Nagel, Neumann-Neander-Str 6-8 D 52355 Düren, Germany) and genotyping was performed by polymerase chain reaction (PCR) with a specific pair of primers including a sense primer (5'TTG AAC TCA TCG ACC TGC AGG CAT 3') flanking the upstream albumin promoter and an antisense primer (5' GCC TTC TCG AAG CTC TCC TTG TCC3') inside the human *Pim-3* cDNA. Transgenic founder animals were mated with C57BL/6 mice (Charles River Japan, Yokohama, Japan). The male offspring with a heterozygous transgene were used as a transgenic group, while those without a transgene were used as a littermate control. All mice were kept under the specific pathogen-free conditions, and all animal experiments in this study complied with the Guidelines of the Care and Use of Laboratory Animals of Kanazawa University.

Hepatocyte isolation

Mouse hepatocytes were isolated by using a two-step perfusion method with some modifications. Briefly, under anesthetization with Avertin (2,2,2-tribromoethanol, Sigma-Aldrich), a needle was inserted along the inferior vena cava and the liver was perfused sequentially with PBS buffer and collagenase-containing buffer at a rate of 5 - 10 ml/min. The liver was then dissected, suspended in ice-cold PBS, and filtered through a cell strainer with a pore size of 100 μm to remove connective tissue debris and cell clumps. After the cell suspensions were left on ice for 15 min, the resultant precipitates were harvested, suspended in DMEM medium (Sigma-Aldrich) and centrifuged at 800 rpm for 2

min. The cell suspensions were further centrifuged in 45 % Percoll solution (Sigma-Aldrich) at 1,000 rpm for 10 min. The obtained cells were confirmed to consist of more than 95 % hepatocytes based on morphological criteria with a viability of higher than 90 % on trypan blue exclusion test. Purified hepatocytes were used for the following DNA content analysis and immunoblotting analysis.

Cell cycle analysis

The obtained hepatocytes were fixed with 70 % ethanol at -20^{o}C. The fixed cells were incubated with 50 μg/ml propidium iodine (Molecular Probes, Eugene, Oregon) and 1 μg/ml RNase A for 30 min at room temperature. DNA content was then analyzed on a FACS Calibur system (BD Biosciences, Bedford, MA). The distribution of cells in each cell-cycle phase was determined by cell ModFit LT Software (BD Biosciences).

Protein extraction and Western Blotting

Hepatocytes or liver tissues were obtained and homogenized with RIPA buffer (Santa Cruz Biotechnology, Santa Cruz, CA) containing proteinase inhibitor cocktail (Roche Diagnostics AG, Rotkreutz, Switzerland). After sonication for 1 min, homogenates were centrifuged at 15,000 x g for 15 min at 4^{o}C, to obtain the supernatants. After total protein concentrations were measured using a BCA kit (Pierce Biotechnology, Rockford, IL), the resultant supernatants were subjected to immunoblotting using anti-phospho-Ser^{112}-Bad, anti-phospho-Ser^{136}-Bad, anti-Bad, anti-Pim-3, anti-β actin (Sigma-Aldrich), and anti-cyclin D1 (Cell Signaling Technology, Beverly, MA), and anti-PCNA antibodies (BD Biosciences) as previously described (Li *et al.,* 2006).

Chemical-induced liver injury and subsequent hepatocarcinogenesis

Three-week old weaning mice were given a single intraperitoneal injection of DEN (Sigma-Aldrich, St, Louis, MO), dissolved in physiological saline solution at a dose 10 mg/kg body weight as previously described (Yang *et al.*, 2006) to induce hepatocarcinogenesis. In order to induce acute liver injury, mice were given a dose of 100

mg/kg body weight. Serum alanine amino transferase (ALT) levels were determined using a Fuji DRICHEM 55500V (Fuji Medical System, Tokyo, Japan) according to the manufacturer's instructions. Mice were sacrificed at the indicated time intervals after the injection to conduct histopathological analysis.

RNA isolation and RT-PCR

Total RNAs were extracted from organs using RNeasy mini kit (Qiagen) according to the manufacturer's instructions and were further treated with RNase-free DNase (Promega) to deplete residual contaminated DNA. Two μg of RNA was reverse-transcribed at 42^{o}C for 1 h in 20 μl reaction mixture containing Moloney murine leukemia virus reverse trancriptase (Toyobo, Osaka, Japan) and hexanucleotide random primer (Qiagen) to obtain cDNA as previously described (Wu *et al.*, 2008). Serially 2-fold diluted cDNA products were amplified for GAPDH using a specific set of primers (Table 1) with 25 cycles consisting of 94^{o}C for 30 s, 58^{o}C for 30 s and 72^{o}C for 1 min in a 25 μl of reaction mixture containing Taq polymerase (Takara Bio, Kyoto, Japan) to evaluate the quantity of the transcribed cDNA. Equal quantities of cDNA products were then amplified for the indicated genes using the specific sets of primers (Table 1) with 35 cycles consisting of 94^{o}C for 30 s, 58^{o}C for 1 min and 72^{o}C for 1 min. The resultant PCR products were fractionated on 1.5% agarose gel and visualized by ethidium bromide staining under ultraviolet light transillumination. The band intensities were measured using NIH Image analysis software version 1.62, and the ratios to GAPDH were calculated on the assumption that the ratios of untreated animals were set at 1.0.

Histopathological analysis

The liver tissue was fixed in 10 % formalin buffered with PBS (pH 7.2) and embedded in paraffin. Five-μm thick sections were stained with hematoxylin and eosin solution or subjected to the TUNEL assay (MBL Co. Ltd., Nagoya, Japan) according to the manufacturer's instructions. Immunohistochemical analysis was performed using anti-PNCA (BD Biosciences) or anti-cleaved caspase-3 antibodies (Cell Signaling Technology). A

portion of the liver tissue was snap-frozen, then dried at room temperature until the tissues became firmly adherent to the slides and fixed in cold acetone for 10 min. The sections were blocked with Serum-free Protein Block (Dako Cytomation) and were incubated with rabbit anti-cyclin B1 antibodies (Santa Cruz Biotechnology). They were further incubated with Alexa Fluor 488-labeled donkey anti-rabbit IgG followed by counterstaining with DAPI (Vector Laboratories) in dark. Immunoflurescence was visualized on a Carl Zeiss Laser Scanning Microscope 510 and cyclin B1-positive cell proportion was determined on 10 randomly chosen fields at 200-fold magnification. Another slides were used for staining with oil red (Sigma Aldrich) and hematoxylin counterstaining, or immunohistochemical analysis using anti-CD31 antibodies (BD Pharmingen). The immune complexes were visualized by Envision+ System (DAKO Cytomation), a catalyzed signal amplification system (DAKO Cytomation) or the Elite ABC kit and DAB substrate kit (Vector Laboratories) according to the manufacturer's instructions. The positive cell numbers were enumerated on 10 randomly chosen visual fields at ×400 magnification. CD31-postive areas were determined as previously described (Wu et al, 2008). In brief, CD31-positive areas in the tumor tissue were defined as the intratumoral vascular areas. Areas of active neovascularization (hot spot) were found inside tumor foci by scanning the section at lower magnification and the pixel numbers of CD31-positive areas were then determined on 5 randomly chosen fields in hot spots of each animal at 400-fold magnification with the aid of Photoshop version 7.0. The density of neovascularization was expressed as a percentage of the whole tumor area. All histopathological examinations were conducted by an examiner without any prior knowledge of the experimental procedures. All histopathological examinations were conducted blind, by an examiner without any prior knowledge of the experimental procedures.

Statistical analysis

All obtained data were calculated and expressed as mean ± SD. The differences were analyzed statistically using one-way ANOVA, followed by the Turkey-Kramer test. $p<0.05$ was considered statistically significant.

Results

Characterization of transgenic mice overexpressing Pim-3 under the control of the albumin promoter

Pim-3 transgenic mice were born at a Mendelian ratio, were fertile, and did not show any apparent abnormalities in the liver until one year after birth (data not shown). We first examined the expression pattern of Pim-3 in Pim-3 transgenic mice. Mouse *Pim-3* mRNA was detected in liver to a similar extent in both wild-type (WT) and Pim-3 transgenic mice, whereas human *Pim-3* mRNA was exclusively detected in Pim-3 transgenic mice (Figure 1B). Consistently, Pim-3 protein was detected abundantly in liver of Pim-3 transgenic mice but not WT mice (Fig. 1B). Pim-3 protein was also detected in the heart and kidney of Pim-3 transgenic mice, but not WT mice (Fig. 1C). Because anti-Pim-3 recognizes both human and mouse Pim-3 to a similar degree, we further examined the mRNA of human and mouse Pim-3 in liver, heart, and kidney. Human *Pim-3* mRNA was detected in the liver of Pim-3 transgenic mice, but not other organs (Fig. 1D). These observations would indicate that Pim-3 transgenic mice express human Pim-3 abundantly and selectively in liver.

Enhanced hepatocyte proliferation by Pim-3 overexpression

Because Pim-3 can phosphorylate a pro-apoptotic molecule, Bad, at the Ser^{112} residue but not the Ser^{136} residue, we first examined the phosphorylation states of Bad, in order to prove the functionality of the Pim-3 gene, selectively overexpressed in liver. Bad was constitutively phosphorylated at Ser^{112} in hepatocytes from Pim-3 transgenic but not WT mice (Fig. 2A). However, the level of phospho-Ser^{136}-Bad was not enhanced in Pim-3 transgenic mice. These observations would indicate that overexpressed Pim-3 was functional in terms of its capacity to phosphorylate Bad, its substrate. The levels of cyclin D1 and PCNA in hepatocytes were increased in Pim-3 transgenic mice, compared to that observed for WT mice (Fig. 2B). Moreover, cell cycle analysis of isolated heptocytes revealed that the proportion of the cells in subG1 phase, which represent apoptotic cells, was marginally but not significantly decreased in Pim-3 transgenic mice. However, the proportion of the cells in G2/M phase was significantly increased in Pim-3 transgenic mice,

compared to that observed for wild-type mice (Fig. 2C). In order to exclude the possibility that isolation of hepatocytes from liver gave rise to artificially high proportion of cells in G2/M phase, we also enumerated the proportion of cells in G2/M phase by immunostaining liver tissues with anti-cyclin B1 antibodies. The proportion of cyclin B1-positive cells were significantly higher in Pim-3 transgenic mice than WT mice (Fig. 2D). Moreover, TUNEL staining failed to detect any significant differences in the numbers of apoptotic hepatocytes between untreated WT and Pim-3 transgenic mice (Fig. 2E). These observations suggest that Pim-3 overexpressed in liver can accelerate the cell cycle progression of hepatocytes.

Enhanced liver damage in Pim-3 transgenic mice

We then treated Pim-3 transgenic and WT mice with DEN, a potent hepatocarcinogen. Both Pim-3 transgenic and wild-type mice survived exposure to DEN. Serum ALT levels, a marker of liver injury, increased with a maximal levels less than 1,000 IU/L and were significantly but not markedly higher in Pim-3 transgenic mice than WT mice (Fig. 3A). These observations suggest that DEN-induced acute liver injury was mild. This may account for comparable levels of apoptosis in liver after DEN treatment until 72 h after the injection (Fig. 3B and 3C). In contrast, PNCA and cyclin D1 levels were higher at 72 h after the injection in Pim-3 transgenic mice, than that observed for WT mice (Fig. 3D and 3E). Moreover, proliferating cells were progressively increased in the centrilobular region of Pim-3 transgenic mice and to a lesser degree, WT mice (Fig. 3F and 3G). The crucial involvement of TNF-α in hepatocyte proliferation (Yamada *et al.*, 1997) prompted us to determine intrahepatic expression of tumor necrosis factor (TNF)-α mRNA levels. TNF-α mRNA levels were increased significantly at 48 h after DEN treatment (Fig. 3H). These observations indicate that the DEN challenge enhanced liver damage in Pim-3 transgenic mice, compared to that observed for WT mice, despite increased hepatocyte proliferation.

Enhanced hepatocarcinogenesis in Pim-3 transgenic mice

We next examined the changes in liver in the later phase of DEN treatment. Because lipid droplet accumulation precedes the onset of DEN-induced HCC development (Wang *et*

al., 2009), we examined the lipid droplet accumulation in liver after DEN treatment. Lipid droplet accumulation was more evident in Pim-3 transgenic mice than WT mice, until 6 months after DEN treatment (Fig. 4A). PCNA-positive proliferating cell numbers were progressively increased in Pim-3 transgenic mice, and to a lesser degree, WT mice (Fig. 4B and 4C). TNF-α was potentially involved in hepatocarcinogenesis (Roberts *et al.,* 1999; Schwabe *et al.,* 2006). Moreover, its expression was enhanced to a greater extent in Pim-3 transgenic mice than that observed for WT mice promptly after treatment with a high-dose of DEN (Fig. 3H). Hence, we investigated TNF-α mRNA expression in the course of hepatocarcinogenesis, together with other pro-inflammatory cytokines, IL-1. Indeed, TNF-α mRNA expression was enhanced in Pim-3 transgenic and WT mice after DEN treatment, but the increase was more evident in Pim-3 transgenic mice (Fig. 4D). A similar tendency was observed for IL-1β but not IL-1α. Dysplastic cells were observed and lobules were distorted in livers of Pim-3 transgenic mice, but not WT mice 6 months after DEN treatment (Fig. 5A). At 10 months after the injection, nodules consisting of highly dysplastic malignant cells were observed in liver of Pim-3 transgenic mice, and to a lesser extent, WT mice (Fig. 5A). Macroscopically, approximately half of male WT mice developed HCC nodules 10 months after DEN injection (Fig. 5B to 5D), consistent with the previous report (Yang *et al*., 2006). In contrast, most Pim-3 transgenic mice developed HCC nodules by 10 months after DEN treatment, with higher relative liver weight and larger numbers of HCC nodules than WT mice (Figure 5B to 5E). The enhanced hepatocarcinogenesis in Pim-3 transgenic mice may mirror the fact that neovascularization, an essential process for hepatocarcinogenesis, was augmented in Pim-3 transgenic mice compared to that observed for WT mice, as demonstrated by increases in CD31-positive areas in the liver (Fig. 5F and 5G).

Discussion

We previously observed that Pim-3 was expressed selectively in pre-malignant and malignant lesions of the mouse HCC model in HBV surface antigen transgenic mice (Fujii *et al.*, 2005). Moreover, Pim-3 protein was detected in a substantial proportion of HCC cells and precancerous lesions in human liver samples, but not normal human liver. Furthermore, Pim-3 protein was also detected in regenerating bile ductules, which are assumed to be the proliferation of hepatic stem cells after chronic injury. These observations suggested potential roles of aberrantly expressed Pim-3 in hepatocarcinogenesis. In order to address the roles of Pim-3, we prepared transgenic mice, which constitutively express human Pim-3 selectively in liver. Untreated hepatocytes derived from these transgenic mice exhibited enhanced cell proliferation, compared to those obtained from WT mice. However, these transgenic mice did not develop HCC spontaneously. Hence, enhanced cell proliferation cannot per se result in carcinogenesis in liver.

Kinase activation generally requires a post-translational modification, particularly, phosphorylation in its regulatory domain. However, another member of the Pim kinase family, Pim-1, is constitutively active without any further alteration in its conformation, because it lacks any regulatory domain (Qian *et al.*, 2005). Likewise, Pim-3 lacks any regulatory domain (Fujii *et al.*, 2005) and *Pim-3* cDNA alone induced phosphorylation of its target protein, Bad, at Ser^{112} when it was transfected into human pancreatic cancer cell lines (Li *et al.*, 2006). Consistently, Pim-3 transgenic mice exhibited enhanced phosphorylation of Bad at Ser^{112} in the liver. The proapoptotic activity of Bad is regulated by its phosphorylation at Ser^{112} or Ser^{136} (She *et al.*, 2005). Unphosphorylated Bad binds and eventually inactivates anti-apoptotic family members, primarily Bcl-X_L but also Bcl-2 (Yang *et al.*, 1995; Zha *et al.*, 1996). Because phosphorylation of Bad at Ser^{112} or Ser^{136} can result in the liberation of Bcl-X_L and Bcl-2, which can prevent apoptosis (Chen *et al.*, 2005), phosphorylated Bad represents its inactive form. However, both WT and Pim-3 transgenic mice developed apoptosis in liver to a similar extent, when they were treated with a potent hepatocarcinogen, DEN. These observations suggest that phosphorylated Bad

is not sufficient to prevent apoptosis induced by potent hepato-cytotoxic drugs such as DEN.

Pim-3 transgenic mice developed HCC with a higher incidence and a heavier burden, than wild-type mice when both were treated similarly with DEN. Hepatocytes, particularly those in the centrilobular region, metabolized DEN into an alkylating agent, which, in turn, can induce DNA damage and mutations in hepatocytes (Verna *et al.*, 1996). Simultaneously, DEN metabolites can generate reactive oxygen species (ROS) (Kamata *et al.*, 2005; Schwabe and Brenner, 2006). When treated with DEN, mice with liver-specific deletion of an essential kinase for NF-κB activation, IKKβ, generated increased levels of ROS in hepatocytes, together with enhanced hepatocyte death and augmented compensatory hepatocyte proliferation. The net result was exaggerated HCC development with a high cell proliferation rate as evidenced by increased PCNA- and cyclin D1-positive cell numbers in liver (Maeda *et al.*, 2005). Likewise, DEN treatment augmented hepatocyte proliferation but not apoptosis in Pim-3 transgenic mice, compared to that observed wild-type mice, as evidenced by increased PCNA- and cyclin D1-positive cell numbers in liver. These data may account for accelerated hepatocarcinogenesis in Pim-3 transgenic mice. However, several lines of evidence indicate the potential involvement of other Pim kinases, Pim-1 and Pim-2, in NF-κB activation (Hammerman *et al.,* 2004; Zemskova *et al.*, 2008). Thus, it still remains to be investigated whether the Pim-3 transgene can induce ROS generation in a similar fashion as the IKKβ deletion.

Liver injury causes liver regeneration primarily through hepatocyte division but if hepatocyte division is impaired, liver repair requires the recruitment of hepatic oval cells (Ma *et al.*, 2006). Oval cells mainly express α-fetoprotein but not albumin, and can proliferate and differentiate into both hepatocytes and bile duct cells. Several independent groups claimed that HCC cells can arise from oval cells (Braun *et al.*, 1989). Mice deficient in the *IKKβ* gene in liver, developed HCC with a higher incidence than wild-type mice (Maeda *et al.*, 2005). In this mouse, the *IKKβ* gene was deleted by using cre recombinase expressed under the control of an albumin promoter/enhancer and therefore, the gene was deleted selectively in albumin-expressing hepatocytes but not oval cells. Because we

utilized the same promoter/enhancer to prepare transgenic mice, it is likely that the Pim-3 transgene was expressed selectively in hepatocytes but not oval cells. Thus, the Pim-3 transgene mainly acted on hepatocytes to promote carcinogenesis, although its effects on oval cell proliferation cannot completely be excluded.

Accumulating evidence indicates that Pim-1, a member of the Pim kinase family, can progress cell cycle by phosphorylating several cell cycle regulators and altering their activities. Pim-1 can phosphorylate the phosphatase Cdc25A, thereby increasing its phosphatase activity (Mochizuki *et al.*, 1999). Moreover, Pim-1 can phosphorylate G1-specific inhibitor p21 (Waf), a cyclin-dependent kinase inhibitor, and induce its cytoplasmic localization (Wang *et al.*, 2002). Furthermore, Pim-1 can phosphorylate the kinase Cdc25C-associated kinase (C-TAK) 1 and decrease its kinase activity (Bachmann *et al.*, 2004), while Pim-1 can phosphorylate and activate the G2/M specific phosphatase Cdc25C. Alteration of the activities of these molecules can result in cell cycle progression, particularly at the G2/M phase. Pim-3 and Pim-1 but not Pim-2 bind to a consensus peptide substrate (AKRRRHPSGPPTA) with a striking high affinity, having Kd value in the range of 40 to 60 nM (Bullock *et al.*, 2005). Thus, it is likely that Pim-3 can phosphorylate these cell cycle regulators similarly as Pim-1. Supporting this notion, recombinant Pim-3 protein can phosphorylate p21/Waf *in vitro* (Morishita *et al.*, 2008). This may account for the observations that cell cycle progression was accelerated in Pim-3 transgenic mouse-derived hepatocytes, compared to wild-type mice, as evidenced by increased proportion of the cells in G2/M phase and reciprocally decreased proportion of the cells in G0/G1 phase.

DEN induced TNF-α production consistently with the previous report (Sakurai *et al.*, 2006) and the production was further augmented by Pim-3 overexpression in liver. The crucial involvement of TNF-α in hepatocyte proliferation was proposed by the observation that liver regeneration after partial hepatectomy was impaired in mice deficient in TNF receptor gene (Yamada *et al.*, 1997). Moreover, accumulating evidence indicates the potential contribution of TNF-α to hepatocarcinogenesis (Roberts et al., 1999; Schwabe et al., 2006). Furthermore, TNF-α can promote angiogenesis, an essential process for tumorigenesis, by inducing the production of angiogenic factors such as vascular

endothelial growth factor and hepatocyte growth factor (Yoshida *et al.*, 1997; Tamura *et al.,* 1993). TNF-α production was regulated at several steps, and the first one is at the transcription levels governed by transcription factors such as NF-κB and AP-1 (Chung *et al.*, 2007; Manna *et al.*, 2000; Udalova and Kwiatkowski, 2001). Because Pim-1 can enhance NF-κB transcriptional activity (Zemskova *et al.*, 2008), Pim-3 might be able to similarly activate NF-κB, thereby inducing TNF-α expression.

It is most likely that our transgenic mice expressed a high level of the Pim-3 transgene selectively in hepatocytes. A strong similarity of Pim-3 with another Pim kinase, Pim-1, suggests that Pim-3 can phosphorylate several cell cycle regulators and accelerate cell cycle progression as Pim-1 can. Supporting this notion, we observed enhanced cell cycle progression in untreated Pim-3 transgenic mouse-derived hepatocytes, compared to that observed for WT mice. However, as evidenced by the absence of spontaneous HCC development in Pim-3 transgenic mice, accelerated hepatocyte proliferation alone cannot induce HCC. DEN can generate O^6-methlguanine and induce frequently G-C to A-T transition mutations in hepatocytes (Nakatsuru *et al.*, 1993). The Pim-3 transgene can enhance proliferation of hepatocytes with G-C to A-T transition mutations, thereby accelerating HCC development. We previously observed that Pim-3 expression was detected in pre-malignant and malignant lesions but not normal tissues of liver in humans and mice (Fujii *et al.,* 2005). Thus, Pim-3 may be a promoter but not an initiator of HCC development, and blocking of Pim-3 activity can delay and/or prevent HCC development.

References

Bachmann M, Hennemann H, Xing PX, Hoffmann I, Moroy T (2004). The oncogenic serine/threonine kinase Pim-1 phosphorylates and inhibits the activity of Cdc25C-associated kinase (C-TAK-1): a novel role for Pim-1 at the G2/M cell cycle checkpoint. *J Biol Chem* **279:** 48319-28.

Braun L, Mikumo R, Fausto N (1989). Production of hepatocellular carcinoma by oval cells: cell cycle expression of c-myc and p53 at different stages of oval cell transformation. *Cancer Res* **49:** 1554-61.

Bullock AN, Debreczeni J, Amos AL, Knapp S, Turk BE (2005). Structure and substrate specificity of the Pim-1 kinase. *J Biol Chem* **280:** 41675-82.

Chen L, Willis SN, Wei A, Smith BJ, Fletcher JI, Hinds MG *et al* (2005). Differential targeting of prosurvival Bcl-2 proteins by their BH3-only ligands allows complementary apoptotic function. *Mol Cell* **17:** 393-403.

Chung J, Koyama T, Ohsawa M, Shibamiya A, Hoshi A, Hirosawa S (2007). 1,25(OH)(2)D(3) blocks TNF-induced monocytic tissue factor expression by inhibition of transcription factors AP-1 and NF-kappaB. *Lab Invest* **87:** 540-7.

Deneen B, Welford SM, Ho T, Hernandez F, Kurland I, Denny CT (2003). PIM3 proto-oncogene kinase is a common transcriptional target of divergent EWS/ETS oncoproteins. *Mol Cell Biol* **23:** 3897-908.

Farazi PA, DePinho RA (2006). Hepatocellular carcinoma pathogenesis: from genes to environment. *Nat Rev Cancer* **6:** 674-87.

Feldman JD, Vician L, Crispino M, Tocco G, Marcheselli VL, Bazan NG *et al* (1998). KID-1, a protein kinase induced by depolarization in brain. *J Biol Chem* **273:** 16535-43.

Fujii C, Nakamoto Y, Lu P, Tsuneyama K, Popivanova BK, Kaneko S *et al* (2005). Aberrant expression of serine/threonine kinase Pim-3 in hepatocellular carcinoma development and its role in the proliferation of human hepatoma cell lines. *Int J Cancer* **114:** 209-18.

Hammerman PS, Fox CJ, Cinalli RM, Xu A, Wagner JD, Lindsten T *et al* (2004). Lymphocyte transformation by Pim-2 is dependent on nuclear κB activation. *Cancer Res* **64:** 8341-8.

Hosono S, Chou MJ, Lee CS, Shih C (1993). Infrequent mutation of p53 gene in hepatitis B virus positive primary hepatocellular carcinomas. *Oncogene* **8:** 491-6.

Kamata H, Honda S, Maeda S, Chang L, Hirata H, Karin M (2005). Reactive oxygen species promote TNFalpha-induced death and sustained JNK activation by inhibiting MAP kinase phosphatases. *Cell* **120:** 649-61.

Li YY, Popivanova BK, Nagai Y, Ishikura H, Fujii C, Mukaida N (2006). Pim-3, a proto-oncogene with serine/threonine kinase activity, is aberrantly expressed in human pancreatic cancer and phosphorylates bad to block bad-mediated apoptosis in human pancreatic cancer cell lines. *Cancer Res* **66:** 6741-7.

Ma W, Xia X, Stafford LJ, Yu C, Wang F, LeSage G *et al* (2006). Expression of GCIP in transgenic mice decreases susceptibility to chemical hepatocarcinogenesis. *Oncogene* **25:** 4207-16.

Maeda S, Kamata H, Luo JL, Leffert H, Karin M (2005). IKKbeta couples hepatocyte

death to cytokine-driven compensatory proliferation that promotes chemical hepatocarcinogenesis. *Cell* **121:** 977-90.

Manna SK, Mukhopadhyay A, Aggarwal BB (2000). Leflunomide suppresses TNF-induced cellular responses: effects on NF-kappa B, activator protein-1, c-Jun N-terminal protein kinase, and apoptosis. *J Immunol* **165:** 5962-9.

Mochizuki T, Kitanaka C, Noguchi K, Muramatsu T, Asai A, Kuchino Y (1999). Physical and functional interactions between Pim-1 kinase and Cdc25A phosphatase. Implications for the Pim-1-mediated activation of the c-Myc signaling pathway. *J Biol Chem* **274:** 18659-66.

Morishita D, Katayama R, Sekimizu K, Tsuruo T, Fujita N (2008). Pim kinases promote cell cycle progression by phosphorylating and down-regulating p27Kip1 at the transcriptional and posttranscriptional levels. *Cancer Res* **68:** 5076-85.

Nakatsuru Y, Matsukuma S, Nemoto N, Sugano H, Sekiguchi M, Ishikawa T (1993). O^6-methylguanine-DNA methyltransgerase protects against nitrosamine-induced hepatocarcinogenesis. *Proc Natl Acad Sci USA* **90:** 6468-72.

Otani K, Korenaga M, Beard MR, Li K, Qian T, Showalter LA *et al* (2005). Hepatitis C virus core protein, cytochrome P450 2E1, and alcohol produce combined mitochondrial injury and cytotoxicity in hepatoma cells. *Gastroenterology* **128:** 96-107.

Pinkert CA, Ornitz DM, Brinster RL, Palmiter RD (1987). An albumin enhancer located 10 kb upstream functions along with its promoter to direct efficient, liver-specific expression in transgenic mice. *Genes Dev* **1:** 268-76.

Popivanova BK, Li YY, Zheng H, Omura K, Fujii C, Tsuneyama K *et al* (2007).

Proto-oncogene, Pim-3 with serine/threonine kinase activity, is aberrantly expressed in human colon cancer cells and can prevent Bad-mediated apoptosis. *Cancer Sci* **98:** 321-8.

Qian KC, Wang L, Hickey ER, Studts J, Barringer K, Peng C *et al* (2005). Structural basis of constitutive activity and a unique nucleotide binding mode of human Pim-1 kinase. *J Biol Chem* **280:** 6130-7.

Roberts RA, Kimber I (1999). Cytokines in genotoxic hepatocarcinogenesis. Carcinogenesis **20**: 1297-401

Sakurai T, Maeda S, Chang L, Karin M (2006). Loss of hepatic NF-kappa B activity enhances chemical hepatocarcinogenesis through sustained c-Jun N-terminal kinase 1 activation. *Proc Natl Acad Sci U S A* **103:** 10544-51.

Schwabe RF, Brenner DA (2006). Mechanisms of Liver Injury. I. TNF-alpha-induced liver injury: role of IKK, JNK, and ROS pathways. *Am J Physiol Gastrointest Liver Physiol* **290:** G583-9.

She QB, Solit DB, Ye Q, O'Reilly KE, Lobo J, Rosen N (2005). The BAD protein integrates survival signaling by EGFR/MAPK and PI3K/Akt kinase pathways in PTEN-deficient tumor cells. *Cancer Cell* **8:** 287-97.

Tamura M, Arakaki N, Tsuboushi H, Takada H, Daikuhara Y. (1993). Enhancement of human hepatocyte growth factor production by interleukin-1α and -1β and tumor necrosis factor-α by fibroblasts in culture. *J Biol Chem* **268**: 8140-5.

Thorgeirsson SS, Grisham JW (2002). Molecular pathogenesis of human hepatocellular carcinoma. *Nat Genet* **31:** 339-46.

Udalova IA, Kwiatkowski D (2001). Interaction of AP-1 with a cluster of NF-kappa B binding elements in the human TNF promoter region. *Biochem Biophys Res Commun* **289:** 25-33.

Umemura T, Ichijo T, Yoshizawa K, Tanaka E, Kiyosawa K (2009). Epidemiology of hepatocellular carcinoma in Japan. *J Gastroenterol* **44 Suppl 19:** 102-107.

Verna L, Whysner J, Williams GM (1996). N-nitrosodiethylamine mechanistic data and risk assessment: bioactivation, DNA-adduct formation, mutagenicity, and tumor initiation. *Pharmacol Ther* **71:** 57-81.

Wang Y, Ausman LM, Geenberg AS, Russel RM, Wang X-D. (2009). Nonalcoholic steatohepatitis induced by a high-fat diet promotes diethylnitrosamine-initiated early hepatocarcinogenesis in rats. *In t J Cancer* **124**: 540-6.

Wang Z, Bhattacharya N, Mixter PF, Wei W, Sedivy J, Magnuson NS (2002). Phosphorylation of the cell cycle inhibitor p21Cip1/WAF1 by Pim-1 kinase. *Biochim Biophys Acta* **1593:** 45-55.

Wu Y, Li YY, Matsushima K, Baba T, Mukaida N (2008). CCL3-CCR5 axis regulates intratumoral accumulation of leukocytes and fibroblasts and promotes angiogenesis in murine lung metastasis process. *J Immunol* **181:** 6384-93.

Yamada Y, Kirillova I, Peschon JJ, Fausto N (1997). Initiation of liver growth by tumor necrosis factor: deficient liver regeneration in mice lacking type I tumor necrosis factor receptor. *Proc Natl Acad Sci U S A* **94:** 1441-6.

Yang E, Zha J, Jockel J, Boise LH, Thompson CB, Korsmeyer SJ (1995). Bad, a heterodimeric partner for Bcl-XL and Bcl-2, displaces Bax and promotes cell death. *Cell*

80: 285-91.

Yang X, Lu P, Fujii C, Nakamoto Y, Gao JL, Kaneko S *et al* (2006). Essential contribution of a chemokine, CCL3, and its receptor, CCR1, to hepatocellular carcinoma progression. *Int J Cancer* **118:** 1869-76.

Yoshida S, Ono M, Shono T, Izumi H, Ishibashi T, Suzuki H *et al* (1997). Involvement of interleukin-8, vascular endothelial growth factor, and basic fibroblast growth factor in tumor necrosis factor α-dependent angiogenesis. *Mol Cell Biol* **17**: 4015-23.

Zemskova M, Sahakian E, Bashkirova S, Lilly M (2008). The PIM1 kinase is a critical component of a survival pathway activated by docetaxel and promotes survival of docetaxel-treated prostate cancer cells. *J Biol Chem* **283:** 20635-44.

Zha J, Harada H, Yang E, Jockel J, Korsmeyer SJ (1996). Serine phosphorylation of death agonist BAD in response to survival factor results in binding to 14-3-3 not BCL-X(L). *Cell* **87:** 619-28.

Zheng HC, Tsuneyama K, Takahashi H, Miwa S, Sugiyama T, Popivanova BK *et al* (2008). Aberrant Pim-3 expression is involved in gastric adenoma-adenocarcinoma sequence and cancer progression. *J Cancer Res Clin Oncol* **134:** 481-8.

Zheng Y, Chen WL, Louie SG, Yen TS, Ou JH (2007). Hepatitis B virus promotes hepatocarcinogenesis in transgenic mice. *Hepatology* **45:** 16-21.

Legends to Figures

Figure 1 Expression of Pim-3 in alb-Pim-3 transgenic mice. A. The schematic representation of the gene used for preparation of Pim-3 transgenic mice. **B.** Expression of human (transgenic) and mouse (endogenous) Pim-3 mRNA and protein levels in liver. The upper three lines are assessed by RT-PCR, while the lower 2 lines are assessed by immunoblotting. Representative results from 5 independent animals are shown here. **C.** Immunoblotting analysis of Pim-3 protein expression in liver, heart, kidney, brain, intestine, spleen, lungs of Pim-3 transgenic mice. The HEK293 cells transfected with human Pim-3 cDNA were used as a positive control. Representative results from 5 independent animals are shown here. **D.** Endogenous mouse Pim-3 mRNA expression in liver, heart and kidney of Pim-3 transgenic mice were determined by RT-PCR. Representative results from 5 independent animals are shown here.

Figure 2 The effects of Pim-3 overexpression on hepatocyte functions. Hepatocytes were obtained from 3-week old WT and Pim-3 transgenic mice and used for the following analyses. **A.** and **B.** Protein was extracted from purified hepatocytes from WT and Tg mice, and was subjected to immunoblotting using anti-phospho-Ser^{112}-Bad, anti-phospho-Ser^{136}-Bad, anti-Bad, anti-cyclin D1, and anti-PCNA antibodies as described in Materials and Methods. Representative results from 4 independent experiments are shown in A. The intensity of each band was determined using NIH Image Analysis software version 1.62 (NIH, Bethesda, MD), and its ratios to β-actin were calculated and are shown in B (n=4). Open boxes, wild-type mice; closed boxes, Pim-3 transgenic mice. **, $p<0.01$. **C.** DNA contents were determined for hepatocytes from WT and Pim-3 transgenic mice as described in Materials and Methods. Representative results from 5 independent experiments are shown here. After the proportion of each fraction was determined, mean and 1 SD were calculated and are shown in the Table (inlet) (n=5). #, $p<0.05$; *, $p<0.01$. **D.** The proportion of cyclin B1-positive cells was determined on liver tissues obtained from 3-week old Pim-3 trangenic and wild-type mice as described in

Materials and Methods. Mean and SEM were calculated (n=6) and are shown here. **E.** The TUNEL assay was conducted as described in Materials and Methods. Representative results from 5 individual animals are shown in the left panel. Positive cells were determined on 5 randomly chosen fields (x 400) from each animal by an examiner without any knowledge of experimental procedures. Mean ± SD are shown in the right panel (n=5).

Figure 3. The effects of overexpressed Pim-3 on apoptosis and cell proliferation after DEN treatment. **A.** Serum ALT levels were determined as described in Materials and Methods. Each symbol indicates serum ALT level of each animal and the bars represent the median of each group. *, $p<0.05$; ** , $p<0.01$ vs. WT mice**. B.** and **C.** Liver tissues were obtained from WT or Tg mice at the indicated time intervals and immunostained with anti-cleaved caspase 3 antibody. Representative results from 5 independent animals are shown in A with an original magnification x 400. Proportion of cleaved caspase 3-positive apoptotic cells were determined as described in Materials and Methods. Mean ± SD are shown in B (n=5). Open boxes, wild-type mice; closed boxes, Pim-3 transgenic mice. **D**. and **E**. Cell lysates were obtained from liver of WT (W) and Pim-3 transgenic mice (T) at 72 h after DEN treatment and subjected to immunoblotting using anti-PCNA or anti-cyclin D1 antibodies. Representative results from 3 independent experiments are shown in D. The intensity of each band was determined and its ratio to β-actin was calculated. Mean ± SD are shown in E (n=5). Open boxes, wild-type mice; closed boxes, Pim-3 transgenic mice. *, $p<0.05$; **, $p<0.01$ vs. WT mice**. F.** and **G.** Liver tissues were obtained from WT or Tg mice at the indicated time intervals and immunostained with anti-PCNA antibody. Representative results from 5 independent animals are shown in G with an original magnification x 400. PCNA-positive proliferating cell numbers were determined as described in Materials and Methods. Mean ± SD are shown in **F** (n=5). *, $p<0.05$; ** , $p<0.01$ vs. WT mice. **H.** Intrahepatic TNF-α mRNA levels were determined as described in Materials and Methods. **, $p<0.01$ vs. WT mice (n=5).

Figure 4. The effects of Pim-3 overexpression in liver pathology in the later phase

after DEN treatment. A. Liver was obtained from WT or Pim-3 transgenic mice (Tg) at the indicated time intervals and was subjected to staining with oil red solution as described in Materials and Methods. Representative results from 5 independent animals are shown with an original magnification x 200. **B**. and **C**. Livers were obtained from WT or Pim-3 transgenic mice at the indicated time intervals and were subjected to immunostaining with anti-PCNA antibody as described in Materials and Methods. Representative results from 5 independent animals are shown in B with an original magnification x 400. PCNA-positive cell numbers were determined as described in Materials and Methods. Mean ± SD are shown in C (n=5). Open boxes, wild-type mice; closed boxes, Pim-3 transgenic mice. *, $p<0.05$; **, $p<0.01$ vs. WT mice. **D, E, and F**. Total RNAs were extracted from liver of WT or Pim-3 transgenic mice at the indicated time intervals after DEN treatment and were subjected to a semi-quantitative RT-PCR analysis for the detection of mRNA of IL-1α (D), IL-1β (E), and TNF-α (F). The ratio of each cytokine was calculated as described in Materials and Methods. Each value represents mean ± SD (n=5). Open boxes, wild-type mice; closed boxes, Pim-3 transgenic mice. *, $p<0.05$; **, $p<0.01$ vs. WT mice.

Figure 5. **Enhanced hepatocarcinogenesis in Pim-3 transgenic mice**. **A.** Liver tissues were obtained from WT or Pim-3 transgenic mice (Tg) at the indicated time intervals after DEN treatment and subjected to HE staining. Representative results from 5 individual animals are shown here with an original magnification x 200. **B**. Macroscopic appearance of liver 10 months and 6 months after DEN treatment. Representative results from 8 animals are shown here. Left panels, Pim-3 transgenic mice; right panels, WT mice. The arrow indicates a small tumor nodule. **C.** Incidence of macroscopic tumor formation at the indicated time intervals after DEN treatment in WT and Pim-3 transgenic mice (Tg). **D.** Liver weight relative to whole body weight was determined on WT and Pim-3 transgenic mice (Tg) at 10 months after DEN treatment. Each value represents mean ± SD (n=5). **, $p<0.01$ vs. WT mice. **E**. Numbers of tumors with a diameter of larger than 1 mm were determined in livers of WT (n=17) or Pim-3 transgenic mice (Tg) (n=16) 10 months after DEN treatment. Each symbol indicates the tumor numbers of each animal and the bars

represent the median of each group. **, $p<0.01$ vs. wild-type mice. **F.** and **G**. Liver tissue were obtained from WT or Pim-3 transgenic mice (Tg) 10 months after DEN treatment and were subjected to immunostaining with anti-CD31 antibody. Representative results from 5 individual animals are shown in F with an original magnification x 400. CD31-positive vascular areas within tumors were determined as described in Materials and Methods. Mean and SD were calculated and are shown in G. *, $p<0.05$ vs. WT mice.

Gene Name	Forward	Reverse	Cycles	Length (bp)
mouse Pim-3	GAGG AGGGTCTCCCCAGAGT	TGGTGGCACGCTTAGGTTG	35	660
human Pim-3	CGGAGGAGGGTCTCTCCAGAGTG	ACCCTGCGCCGGCGGAAAG	35	535
mouse TNF- α	AGTTCTATGGCCCAGACCCT	CGGACTCCGCAAAGTCTAAG	35	463
mouse IL-1 α	CTCTAGAGCTCCATGCTACAGAC	TGGAATCCAGGGGAA ACACTG	35	309
mouse IL-1 β	ATGGCAACTGTTCCTGAACTCAAC T	CAGGACAGGTATAGATTCTTTCCTTTT	35	377
GADPH	ACCACAGTCCATGCCATCAC	TCCACCACCCTGTTGCTGTA	25	431

Table 1. Sequences of the primers used for RT-PCR.

Figure-1

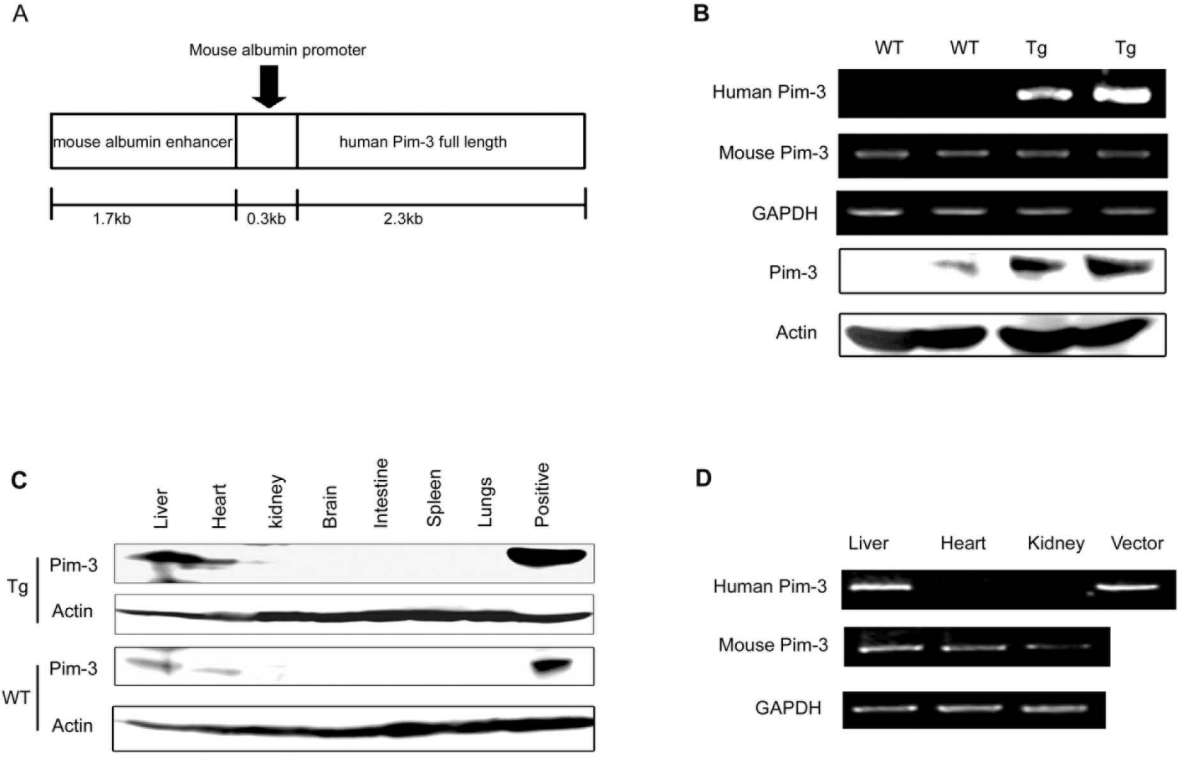
A
Mouse albumin promoter
mouse albumin enhancer
human Pim-3 full length
1.7kb
0.3kb
2.3kb
B
WT
WT
Tg
Tg
Human Pim-3
Mouse Pim-3
GAPDH
Pim-3
Actin
C
Liver
Heart
kidney
Brain
Intestine
Spleen
Lungs
Positive
Tg
Pim-3
Actin
WT
Pim-3
Actin
D
Liver
Heart
Kidney
Vector
Human Pim-3
Mouse Pim-3
GAPDH

Figure 2

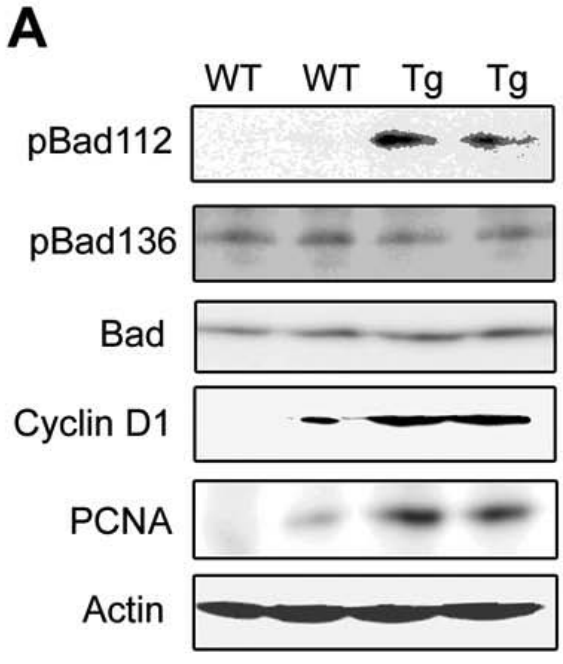

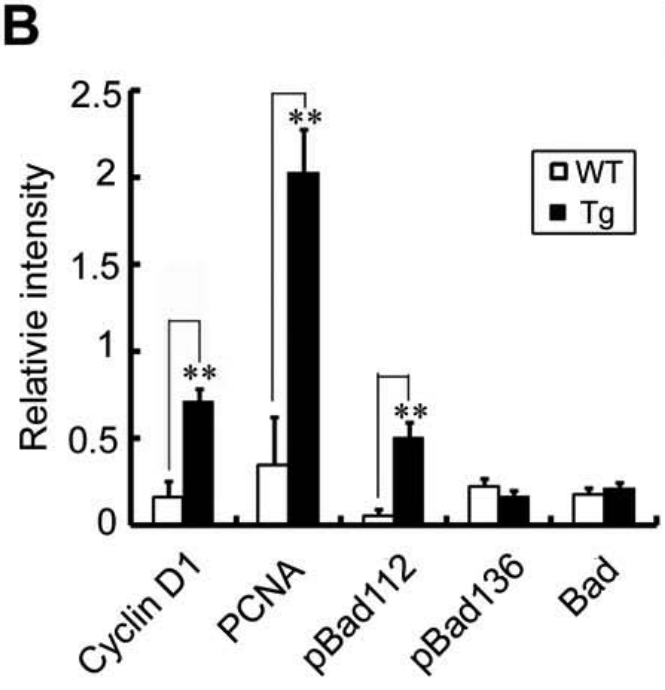

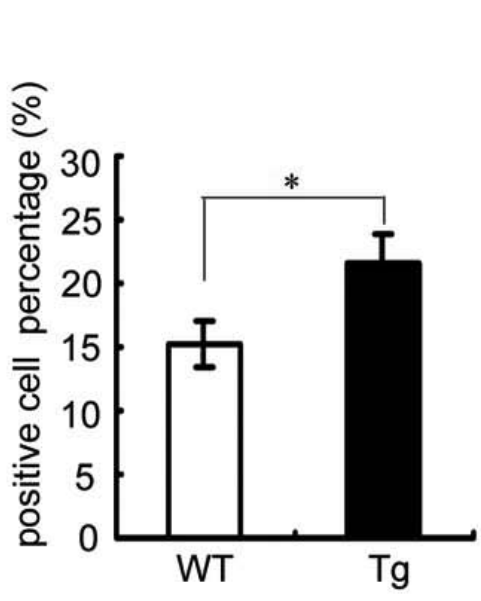

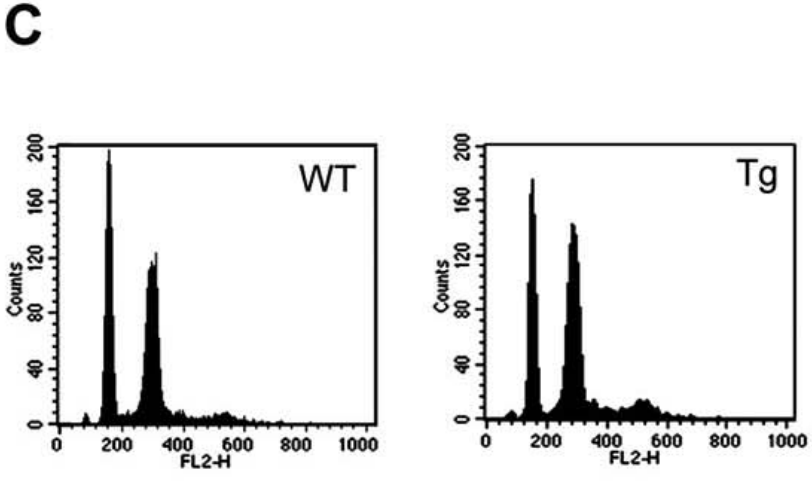

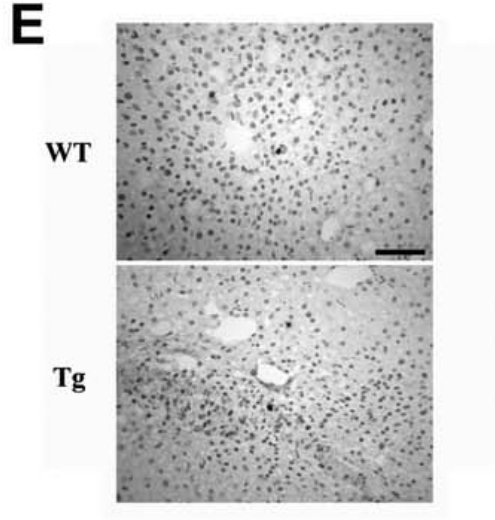

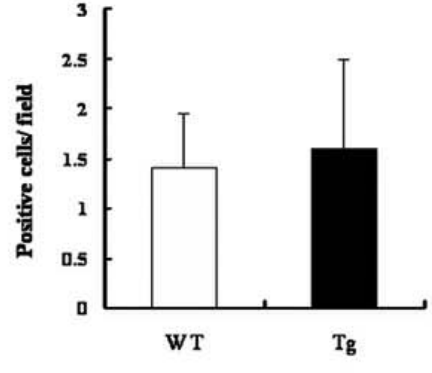

	subG1	G0/G1	S	G2/M	polyploidy
WT	0.87±0.29	40.52±1.12	2.51±0.69	50.40±1.63	5.7±0.54
Tg	0.38±0.12	31.68±0.83*	1.19±0.27	57.19±0.77*	9.55±0.51*

Figure 3

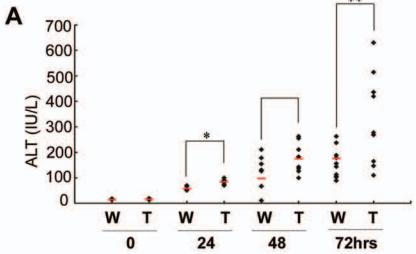
A
ALT (IU/L)
700
600
500
400
300
200
100
0
*
**
W T W T W T W T
0 24 48 72hrs

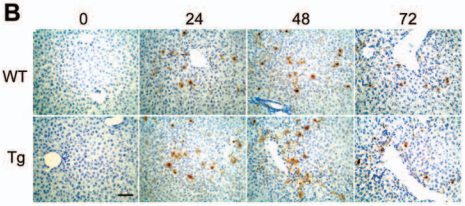
B
0 24 48 72
WT
Tg

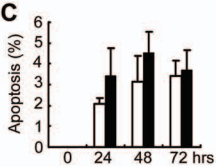
C
Apoptosis (%)
6
5
4
3
2
1
0
0 24 48 72 hrs

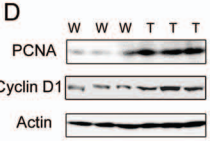
D
W W W T T T
PCNA
Cyclin D1
Actin

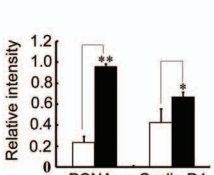
E
Relative intensity
1.2
1.0
0.8
0.6
0.4
0.2
0
**
*
PCNA
Cyclin D1

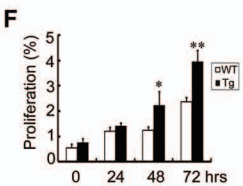
F
Proliferation (%)
5
4
3
2
1
0
*
**
□WT
■Tg
0 24 48 72 hrs

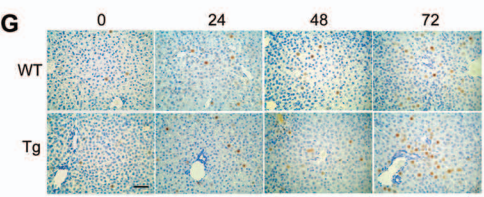
G
0 24 48 72
WT
Tg

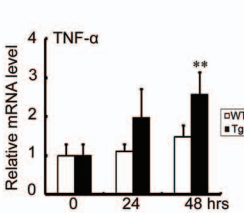
H
TNF-α
Relative mRNA level
4
3
2
1
0
**
□WT
■Tg
0 24 48 hrs

Figure 4

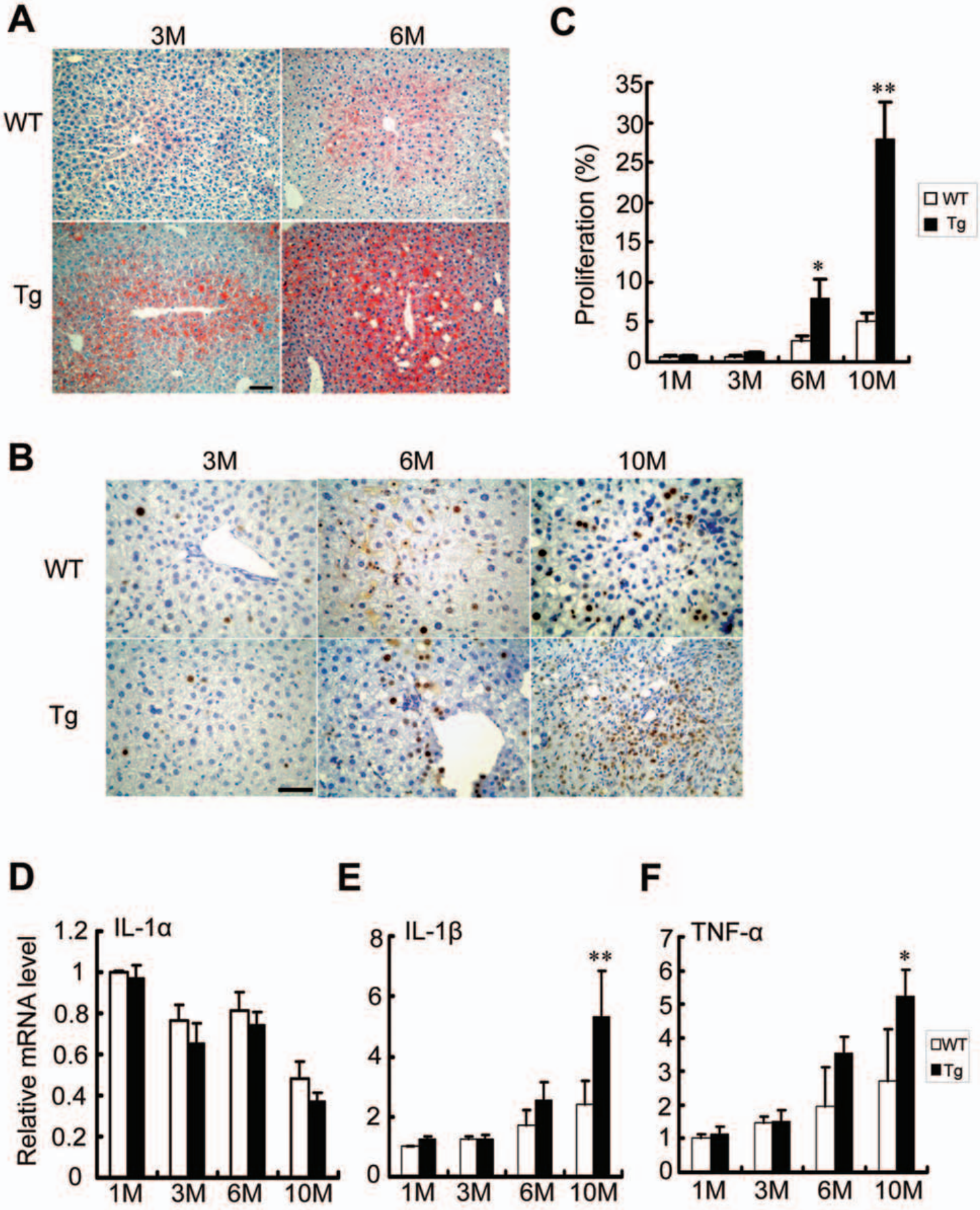
A
3M
6M
WT
Tg
C
Proliferation (%)
35
30
25
20
15
10
5
0
**
*
WT
Tg
1M
3M
6M
10M
B
3M
6M
10M
WT
Tg
D
IL-1α
Relative mRNA level
1.2
1
0.8
0.6
0.4
0.2
0
1M
3M
6M
10M
E
IL-1β
8
6
4
2
0
**
1M
3M
6M
10M
F
TNF-α
7
6
5
4
3
2
1
0
*
WT
Tg
1M
3M
6M
10M

Figure 5

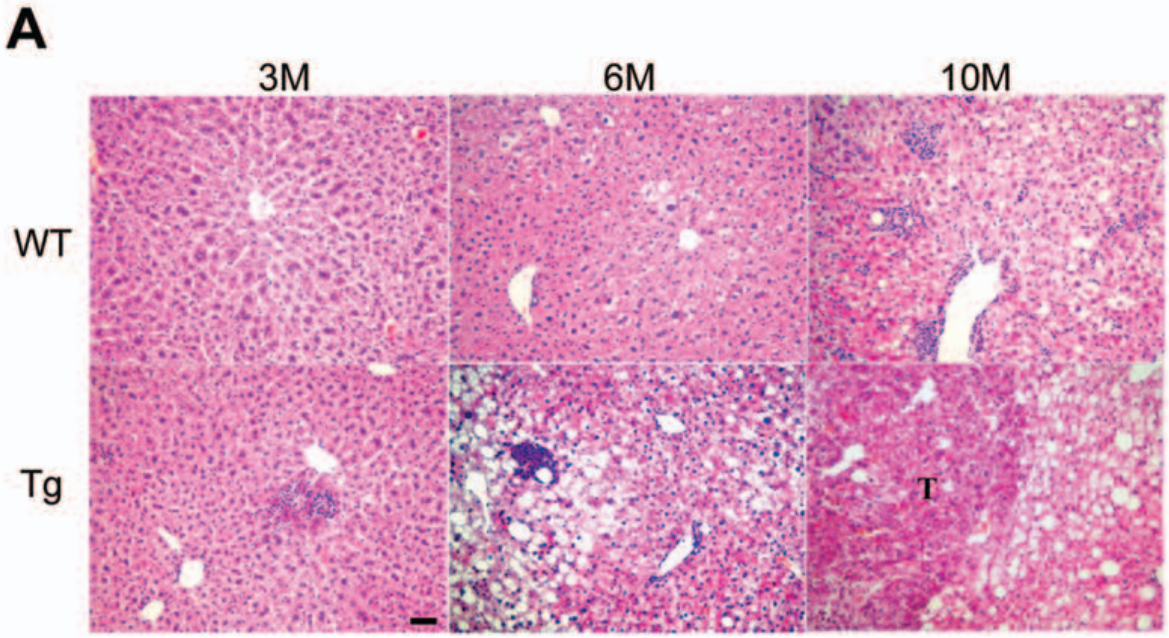

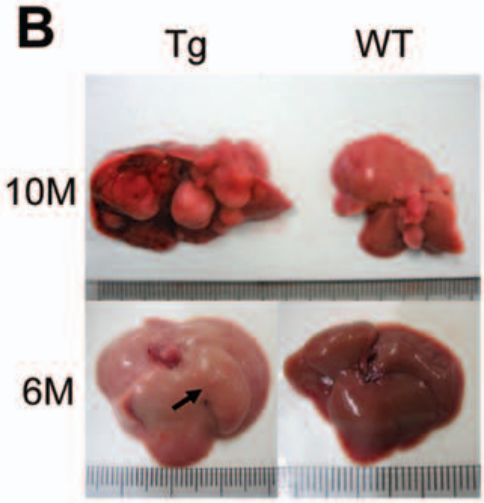

C

	3M	6M	10M
WT	0/7	1/8	7/17
Tg	0/7	3/10	13/16